carbonate (0.75 ml, 5 μmol) resulted in a solution of potassium [^{18}F]fluoride.

[^{18}F]Fluoride dissolved in 66 mM aqueous potassium carbonate (0.75 ml, 5 μmol) was added to a solution of Kryptofix 222 (3.7 mg, 10 μmol; Merck Schuchardt, Hohenbrunn, Germany) in 0.25 ml of acetonitrile. The solvents were removed azeotropically with acetonitrile under a slight flow of helium at 110°C. This procedure was conducted thrice in total with 1.0 ml of dry acetonitrile. Thereafter, Compound **4** (13.5 mg, 20 μmol) in 1.0 ml of dry acetonitrile was added, after which the reaction mixture was heated to 130°C for 5 min (Scheme 2). After cooling to room temperature, 0.24 M sodium ethoxide ethanol solution (1.0 ml, 0.24 mmol) was added, and the reaction mixture was allowed to stand at room temperature for 10 min. The mixture was neutralized by the addition of 1.0 M aqueous sodium acetate (0.3 ml, 0.3 mmol). [^{18}F]NFT202 (**6**) was purified by high-performance liquid chromatography (HPLC) with a preparative column [300×30 (i.d.) mm, Develosil ODS-UG5; Nomura Chemical Co., Ltd., Tokyo, Japan]. The eluent consisted of 25% ethanol in water, and the flow was 6.0 ml/min. The radioactive fraction, eluted with a retention time corresponding to nonradioactive NFT202, synthesized as previously described (companion paper), was collected. After HPLC purification, the solvents were evaporated at 110°C and dissolved in physiological saline solution (decay-corrected radiochemical yield: 81.0±13.9%). The radiochemical purity of the [^{18}F]NFT202-injectable solution was 98.3±1.5%.

2.6. 3′-[^{18}F]3′-Fluoro-3′-deoxythymidine ([^{18}F]FLT)

[^{18}F]FLT was synthesized by a previously published method [2]. The radioactive fraction, eluted with a retention time corresponding to nonradioactive FLT (Sigma-Aldrich Japan KK, Tokyo, Japan), was collected. After HPLC purification, the decay-corrected radiochemical yield was 29.7±7.4%. The radiochemical purity of the [^{18}F]FLT-injectable solution was 95.3±4.0%.

2.7. [^{14}C]NFT202

With 2-fluoroethanol as a starting material, 2-fluoroethyltosylate was synthesized according to the method of Edgell and Parts [3]. 2-Fluoroethyltosylate (6.8 mg, 33.8 μmol), potassium carbonate (9.3 mg, 67.6 μmol) and [^{14}C]Thd (37 MBq, 16.9 μmol) were dissolved in acetone-*N*,*N*-dimethylformamide 1:1 mixed solvent (5 ml), and the mixture was heated at 50°C for 18 h under argon atmosphere. After dilution with 10 ml of diethyl ether, the mixture was loaded onto a short silica gel column (SepPak Silica; Nihon Waters KK). The radioactive product was eluted with 10 ml of chloroform:methanol (5:1). The solvent was removed by evaporation, and the desired product (35.2 MBq, 95%) was purified by silica gel thin-layer chromatography (TLC) (chloroform:methanol=5:1). After TLC purification, the radiochemical purity of [^{14}C]NFT202 was >99%, and specific activity was 2.18 GBq/mmol (according to the specific activity of [^{14}C]Thd).

2.8. Distribution

All procedures were performed in accordance with institutional guidelines (Guidelines for Animal Experiments; University of Fukui, Fukui, Japan). Seven-week-old C57BL/6 mice were purchased from Japan SLC, Inc. (Shizuoka, Japan), and held for 1 week prior to the study. Lewis lung carcinoma (LL/2) cell lines were purchased from Dai-Nippon Seiyaku Co., Ltd. (Osaka, Japan), and were maintained in the recommended culture medium obtained from the manufacturer. The cell lines were grown in a 5% CO_2-humidified atmosphere at 37°C. Tumor-bearing mice were established by subcutaneous injection of 50×10^5 (LL/2) cells to the left shoulder of 8-week-old C57BL/6 mice. The experiments on tumor-bearing mice were performed at least 10 days after inoculation, by which time the tumors had grown to about 5 mm in diameter. A saline solution of 0.1 ml containing 1.85 MBq [^{18}F]-labeled nucleosides was administered as a bolus through the tail vein. The mice were sacrificed by blood removal from the heart under ether anesthesia at predesigned time intervals of 30, 60 and 120 min. Five to six animals were used for each time interval. Urine was collected throughout the experiment, and blood samples were obtained from the syringe used in the sacrifice. Afterwards, tissue samples were removed and weighed together with the blood samples, and urine samples were counted using a 2×2-in. NaI(Tl) scintillator interfaced to a single-channel analyzer autowell gamma counter (Ohyo Koken Kogyo, Tokyo, Japan). The percent dose per organ and the percent dose per of gram tissue were calculated without body weight normalization.

2.9. TK1-dependent cell uptake

A mouse connective tissue cell line (L-M) and its thymidine-kinase-deficient mutant L-M(TK$^-$) cell line were purchased from Dai-Nippon Seiyaku Co., Ltd. and were maintained in the recommended culture media obtained from the manufacturer. The cell lines were grown in a 5% CO_2-humidified atmosphere at 37°C. The L-M(TK$^-$) cell line lacks TK activity [4]. To clarify the TK1-specific incorporation of the nucleoside, we compared the cell uptake of [^{14}C]NFT202 between the L-M and L-M(TK$^-$) cell lines.

The cells were harvested and seeded at a concentration of 2.0×10^5 into 24-well plates, and tracer uptake experiment was performed 24 h after seeding. Thymidine-free Dulbecco's modified Eagle's medium (GIBCO, Grand Island, NY, USA) was used as assay medium. Briefly, 500 μl of assay medium containing 1.3 nmol (around 74 kBq) of each tracer was added to each well, and the plate was incubated at 37°C for 60 min. After incubation, the medium was removed, and the cells were washed thrice with ice-cold phosphate-buffered saline (PBS). After washing, cell lysis was performed with 500 μl of 0.2 N NaOH. After a liquid

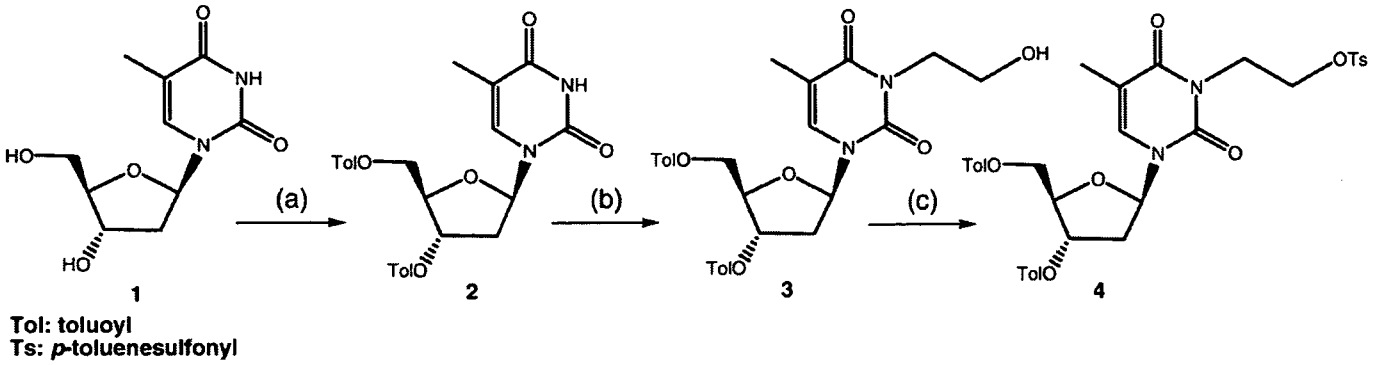

Scheme 1. Synthesis of Compound 4. Conditions: (a) *p*-toluoyl chloride (TolCl), pyridine, room temperature; (b) $BrCH_2CH_2OH$, TBAF, THF, room temperature; (c) *p*-toluenesulfonyl chloride (TsCl), pyridine, 0°C.

scintillator (ACSII; Amersham Biosciences) had been added, radioactivity in the lysate was counted using a liquid scintillation counter (LSC-5000; Aloka, Tokyo, Japan). The protein content of the lysate was then measured with the DCP protein assay reagent (Bio-Rad Japan, Tokyo, Japan). The radioactivity remaining in the wells following cell lysis was less than 5% of the total radioactivity.

2.10. Growth-dependent cell uptake

A549 human lung adenocarcinoma cells were purchased from Dai-Nippon Seiyaku Co., Ltd., and were maintained in the recommended culture medium obtained from the manufacturer. The cell lines were grown in a 5% CO_2-humidified atmosphere at 37°C.

We also compared [^{14}C]NFT202 uptake and cell cycle activity, which was expressed as the S-phase fraction. Toward this end, A549 cells were manipulated to a range of proliferation rates [from actively dividing to growth-arrested (GA)]. For plateau-phase cultures, cells were seeded at the rate of 1.0×10^4 per well in a 24-well plate with 1.0 ml of culture medium and were grown for 8 days with no change of the medium. Under these conditions, 8-day-old cultures show little or no continued growth. To analyze exponentially growing cultures, plateau-phase cultures were released by trypsin treatment and then reseeded in a fresh medium at 2×10^5 cells/well in a 24-well plate. Cell uptake was measured at 6 and 24 h after subculturing into a fresh medium. The results were compared with the uptake of cells that were not subcultured (referred to as GA cell samples).

Cell cycle distributions were determined in parallel cultures by flow cytometry. The cells from five wells were trypsinized and collected in a 15-ml culture tube (Falcon Becton Dickinson, Lincoln Park, NJ, USA). To prepare samples for DNA analysis on a flow cytometer, the cells were sedimented by centrifugation and treated with the CycleTEST PLUS DNA Reagent Kit (Becton Dickinson, San Jose, CA, USA), according to the manufacturer's instructions. The cell cycle profiles of the samples were analyzed by flow cytometry (FACS Calibur; Becton Dickinson), and the S-phase fraction was calculated by Mod-Fit LT software (Becton Dickinson).

2.11. DNA incorporation

[^{14}C]NFT202 incorporation into DNA was measured following the method described by Ayusawa et al. [5]. Briefly, after incubation with [^{14}C]NFT202, A549 cells were washed thrice with ice-cold PBS and treated with 5% trichloroacetic acid, and then the residue was washed with cold 70% ethanol. Both 5% trichloroacetic acid and 70% ethanol were collected and combined as an acid-soluble fraction, then mixed with a liquid scintillation cocktail (ACSII; Amersham Biosciences). The acid-insoluble fraction was dissolved in 0.5 ml of 0.2 N NaOH and then mixed

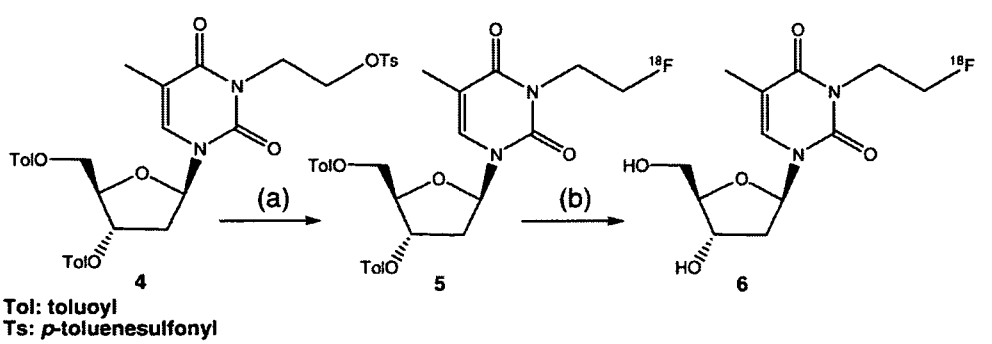

Scheme 2. Radiosynthesis of [^{18}F]NFT202 (**6**). Conditions: (a) $^{18}F^-$, Kryptofix 222, K_2CO_3, CH_3CN, 130°C, 5 min; (b) (i) 0.24 M sodium ethoxide (NaOEt), ethanol (EtOH), room temperature, 10 min; (ii) 1.0 M aqueous sodium acetate; (iii) semiprep HPLC (C-18, 25% EtOH).

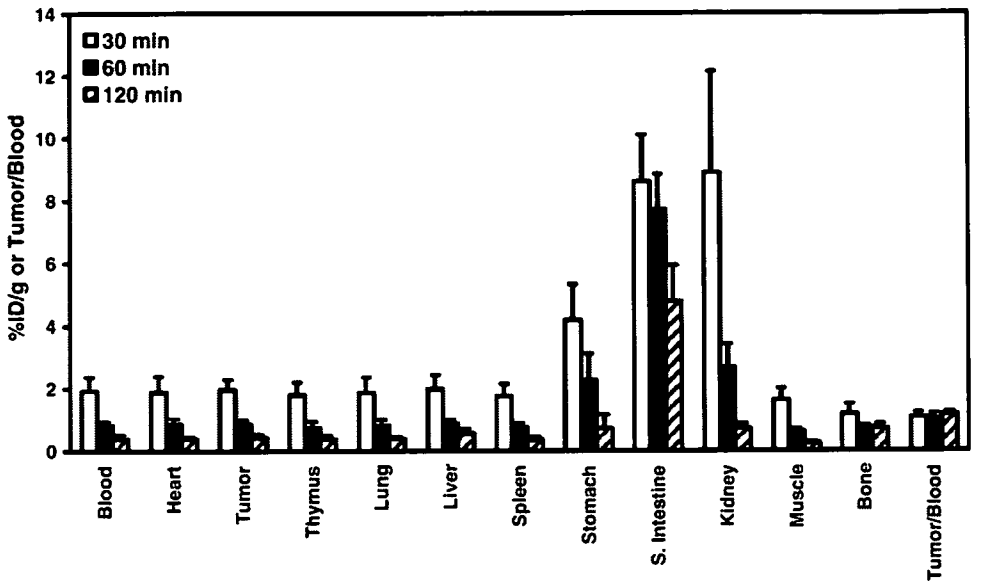

Fig. 1. Tissue distribution of radioactivity (% ID/g) or tumor/blood ratio after intravenous injection of [^{18}F]NFT202 in LL/2-bearing mice. Results are presented as mean±S.D. (n=5).

with a liquid scintillation cocktail (ACSII; Amersham Biosciences). Radioactivity was measured by a liquid scintillation counter (LSC-5100; Aloka).

3. Results

3.1. Synthesis

As outlined in Scheme 1, thymidine (**1**) was protected at the 3′,5′-di-*O*-position with toluoyl chloride in pyridine, yielding Compound **2**. The N^3 alkylation of Compound **2** was conducted in a one-pot reaction from Compound **2** by adapting a procedure described previously [6]. 2-Bromoethanol was added to a solution containing TBAF and Compound **2** in THF at room temperature, providing Compound **3** in high yield (81%). Subsequent activation of the hydroxymethyl group with tosyl chloride in pyridine gave the desired product, Compound **4**. The total yield starting from thymidine was 53%. All compounds were characterized by MS, as well as by ^{1}H and ^{13}C NMR spectroscopy. The purity of the compounds was assessed by the conspicuous absence of impurities in the ^{1}H NMR spectrum, and homogeneity was assessed by TLC.

Radiosynthesis was carried out in a two-step one-pot reaction, as outlined in Scheme 2. The fluorination reaction was conducted according to the method of Hamacher et al. [7].

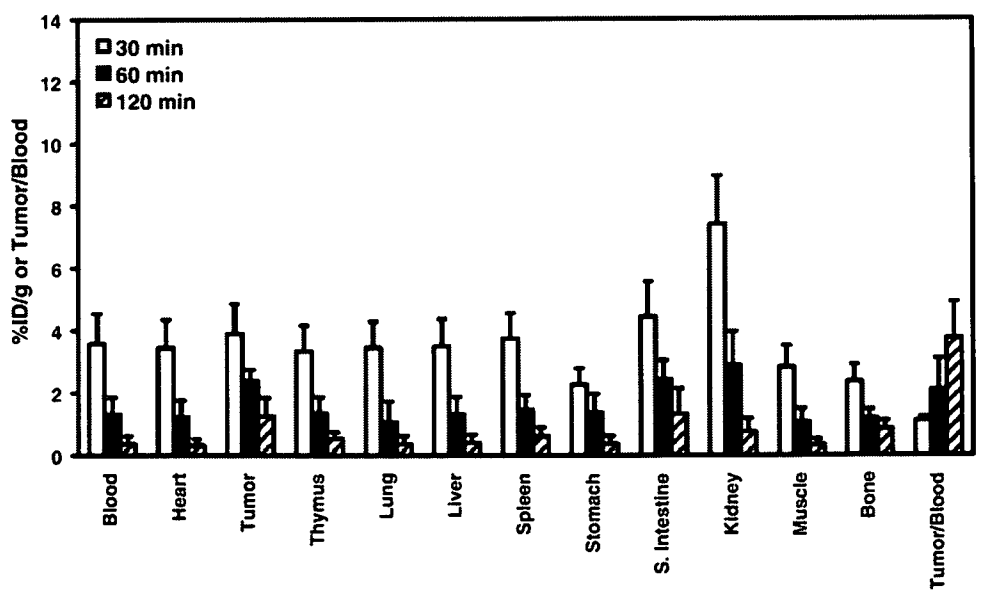

Fig. 2. Tissue distribution of radioactivity (% ID/g) or tumor/blood ratio after intravenous injection of [^{18}F]FLT into LL/2-bearing mice. Results are presented as mean±S.D. (n=5 at 30 and 60 min; n=6 at 120 min).

Thereafter, deprotection was successfully performed with 0.24 M sodium ethoxide at room temperature for 10 min. Following neutralization with 1 M sodium acetate, the crude reaction mixture was purified by HPLC, providing a [^{18}F]NFT202 solution. The decay-corrected radiochemical yield ranged from 65% to 90%. The radiochemical purity of the [^{18}F]NFT202-injectable solution ranged from 97% to 99%.

3.2. Distribution

Figs. 1 and 2 show the tissue distributions of [^{18}F]NFT202 and [^{18}F]FLT in LL/2 tumor-bearing mice, respectively. At 30 min postinjection, radioactivity concentration was lower in the blood of the former than in that of the latter, whereas at 60 min postinjection, the concentrations were the same. [^{18}F]NFT202-injected mice showed renal clearance of radioactivity [87% injected dose (ID) in urine at 120 min postinjection]. There was no significant uptake of radioactivity in the tumors of the [^{18}F]NFT202-injected mice at 120 min postinjection (tumor/blood ratio=1.14, P=.56). However, [^{18}F]FLT-injected mice showed a significantly high radioactivity uptake in the tumors at 120 min postinjection (tumor/blood ratio=3.73, P<.01). Characteristically, the [^{18}F]NFT202-injected mice showed a significantly high radioactivity uptake in the small intestines. The [^{18}F]FLT-injected mice also showed a significantly high radioactivity uptake in the small intestines. However, more radioactivity accumulated in the small intestines of the [^{18}F]NFT202-injected mice than in those of the [^{18}F]FLT-injected mice. There was no significant radioactivity uptake in the thymus or spleen of the [^{18}F]NFT202-injected mice at 120 min postinjection (thymus/blood ratio=0.95, spleen/blood ratio=0.90, P=.64). However, the [^{18}F]FLT-injected mice showed an insignificant uptake in radioactivity in the thymus and spleen at 120 min postinjection (thymus/blood ratio=1.42, P=.20; spleen/blood ratio=1.61, P=.13).

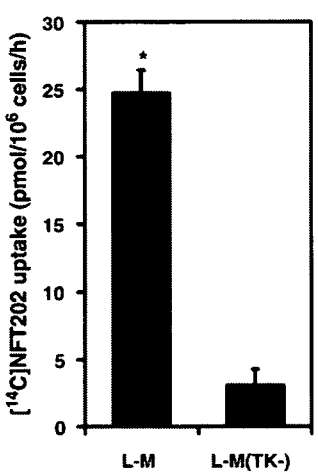

Fig. 3. Cell uptake of [^{14}C]NFT202 between the L-M parent cell and its TK mutant cell line L-M(TK$^-$). *P<.01 compared with L-M(TK$^-$) (Student's t test). Data are expressed as mean±S.D. for three experiments.

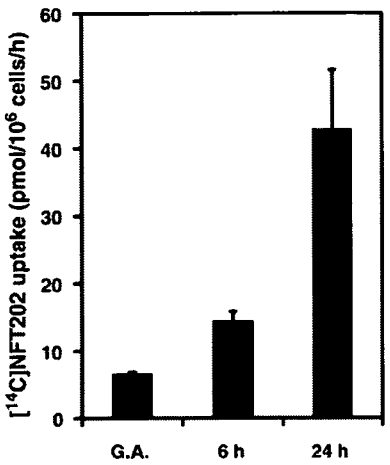

Fig. 4. Growth-dependent cell uptake of [^{14}C]NFT202. [^{14}C]NFT202 uptake was correlated with the S-phase fraction (r^2=.92). The S-phase fraction values of growth arrest, 6 h and 24 h in this experiment were 1.4, 5.1 and 24, respectively. Data are expressed as mean±S.D. for three experiments.

3.3. TK1-dependent cell uptake

The [^{14}C]NFT202 uptake in L-M cells was approximately eight times higher than that in the TK1 mutant L-M(TK$^-$) cells (Fig. 3; P<.01, Student's t test). Therefore, the cell uptake of [^{14}C]NFT202 was clearly TK1-selective.

3.4. Growth-dependent cell uptake

A549 human lung adenocarcinoma cells, with only 1.4% of the cells in the S-phase, took up little [^{14}C]NFT202. When cells were stimulated to grow by placement in a fresh medium, we observed a strong correlation between [^{14}C]NFT202 uptake and the S-phase fraction (Fig. 4; r^2=.92). Fig. 5 compares [^{14}C]FLT and [^{14}C]NFT202 uptake in A549 cells. In the high-density (slow-growth phase) and low-density (active-growth phase) conditions, [^{14}C]FLT uptake was thrice higher than [^{14}C]NFT202 uptake.

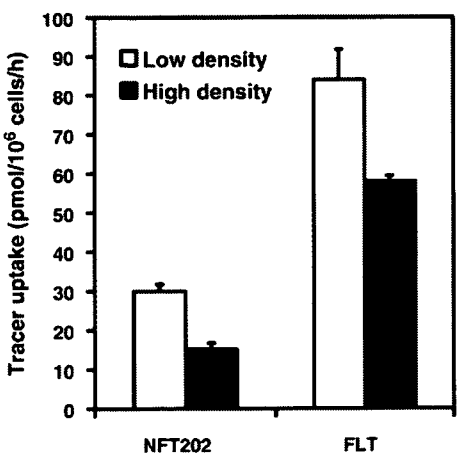

Fig. 5. [^{14}C]FLT and [^{14}C]NFT202 uptake in A549 cells. The high-density cells grew slowly and the low-density cells grew more actively. [^{14}C]FLT uptake was thrice higher than [^{14}C]NFT202 uptake. Data are expressed as mean±S.D. for three experiments.

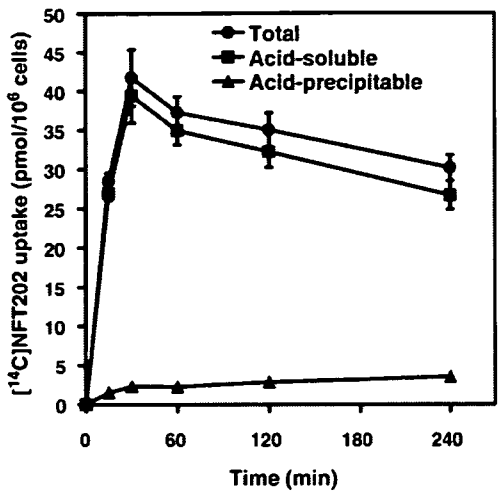

Fig. 6. Time-dependent [^{14}C]NFT202 uptake into A549 lung adenocarcinoma cells. The radioactivity of total, acid-soluble small molecules and acid-precipitable fractions (DNA) is shown. Data are expressed as mean±S.D. for three experiments.

3.5. DNA incorporation

Fig. 6 shows the time-dependent cell uptake and DNA incorporation of [^{14}C]NFT202 in A549 human lung adenocarcinoma cells. The acid-precipitable material from the DNA incorporation assay is DNA. Cellular uptake of [^{14}C]NFT202 increased until 30 min after [^{14}C]NFT202 exposure and then decreased gradually. At 240 min after [^{14}C]NFT202 exposure, the uptake was decreased to 70% of its peak uptake at 30 min. Over 90% of the radioactivity of [^{14}C]NFT202 was found in the acid-soluble fraction. DNA incorporation of [^{14}C]NFT202 was low. The low DNA incorporation was of the same level as that of FLT [8].

4. Discussion

The aim of this study was to evaluate the potential of [^{18}F]NFT202 to serve as a PET ligand for imaging cellular proliferation.

N^3-(2-fluoroethyl)-thymidine (NFT202) has been selected as a candidate cellular proliferation imaging agent because NFT202 is (a) metabolically stable against the degradation reaction of recombinant thymidine phosphorylase; (b) a potent substrate for human TK1; and (c) a high-affinity compound for nucleoside transporter. Therefore, we advanced fluorine-18 labeling of NFT202 and evaluated its suitability as a tracer for cellular proliferation imaging by PET.

Preliminarily, we synthesized three different labeling precursors possessing different 3′,5′-protecting groups (di-*O*-acetyl, di-*O*-toluoyl and di-*O*-tetrahydropyranyl) and evaluated ^{18}F fluorination yield. The best results were achieved with 3′,5′-di-*O*-toluoyl-N^3-(2-*p*-toluenesulfoxyethyl)-thymine (**4**; 81%). The labeling yields of 3′,5′-di-*O*-acetyl-N^3-(2-[^{18}F]fluoroethyl)-thymidine and 3′,5′-di-*O*-tetrahydropyranyl-N^3-(2-[^{18}F]fluoroethyl)-thymidine were 27% and 45%, respectively. Therefore, we selected Compound **4** as a labeling precursor for distribution studies.

In this study, the specific activity of the tracer was not investigated exhaustively. The typical specific activity of the [^{18}F]-labeled compound in our facility was >111 GBq/μmol [9]. In addition, our in vivo experimental system has a significant level of endogenous thymidine, which strongly reduced the in vivo uptake of thymidine analog [10]. Therefore, we evaluated the in vivo potential of [^{18}F]NFT202 by comparing it with [^{18}F]FLT.

In the present in vitro studies using L-M(TK$^-$) cells and growth-manipulated A549 lung carcinoma cells, NFT202 showed TK1-selective and growth-dependent cellular uptake. FLT also shows TK1-dependent and growth-dependent cell uptake [11]. FLT uptake correlated well (r^2=.91) with the increase in the S-phase fraction [11]. Moreover, neither NFT202 nor FLT is effectively incorporated into DNA [8]. In this sense, NFT202 and FLT are similar. However, the net uptake of NFT202 was lower than that of FLT. Moreover, the time-dependent cell uptake of NFT202 showed that NFT202 was finally washed out from the cell. NFT202 possessed the same potential for TK1 phosphorylation and enzymatic stability against TP as FLT, and it was a more suitable substrate than FLT for a nucleoside transporter. Then, what is the difference between NFT202 and FLT? Grierson et al. [1] confirmed that TK1, deoxynucleotidase (dNT) and thymidylate kinase (TMPK) are the main determinants of intracellular FLT retention, and that reversible nucleotide metabolism within the salvage pathway is a significant issue. The DNA salvage pathway involves a futile cycle for nucleoside phosphorylation and dephosphorylation mediated by TK1 and a nucleotidase dNT. This cycle poses an issue for interpreting tracer uptake values, since it provides a mechanism for the loss of established activity in cells. In addition, subsequent phosphorylation of nucleoside monophosphate by other kinases within the DNA synthesis pathway will retain the tracer because the retrograde synthesis of nucleoside from nucleoside triphosphate is thought to be negligible [1]. Therefore, the difference in cell uptake kinetics between NFT202 and FLT might be due to the dephosphorylation kinetics mediated by nucleotidase and to the affinity for other kinases within the DNA synthesis pathway: TMPK and nucleotide diphosphate kinase. These processes (reversible nucleotide metabolism within the salvage pathway) may also influence NFT202 uptake, since they provide a mechanism for the loss of established activity in cells.

The nucleoside efflux pumps also might provide a mechanism for the loss of established activity in cells. MRP8, an ATP-binding cassette transporter associated with P-glycoprotein, is known to extrude 5-fluoro-2′-deoxyuridine monophosphate from cells [12]. Grierson et al. [1] observed a small loss of FLT monophosphate (10%) to media during the efflux experiment, and they recognized that MRP8 nucleotide transporters could mediate this efflux. There is no evidence that MRP8 transports NFT202

monophosphate, but it is worth considering as a way to understand the mechanisms by which NFT202 washes out.

In several ways, our results parallel those of previous validation studies with FLT, in particular uptake/washout studies in A549 cells [1]. These results suggested that an assay for dNT activity and thymidylate kinase activity would have definitively shown which analogs were deserving of further effort.

We preliminarily analyzed the plasma metabolite of the [^{18}F]NFT202-injected mice (data not shown). Plasma radioactivity during the first 30 min was due predominantly to [^{18}F]NFT202 (80%). The intact [^{18}F]NFT202-derived radioactivity in plasma was reduced to 45% at 120 min postinjection. On the other hand, in another tumor-bearing mouse model, plasma radioactivity during the first 60 min was predominantly due to intact [^{18}F]FLT (96%) [13]. Thus, FLT seems to have an advantage in delivery due to higher blood levels. Despite this advantage, FLT shows a tumor/blood advantage only after 60 min. Therefore, tumor delivery of the tracer does not seem to be an important factor in tumor/blood ratio. Barthel et al. [14] reported that in vivo [^{18}F]FLT kinetics depends on TK1 protein expression. However, NFT202 possessed the same potential for TK1 phosphorylation as FLT. The discrepancy in the in vivo efficacy between NFT202 and FLT also may reveal the importance of reversible nucleotide metabolism within the salvage pathway, which determines intracellular nucleoside retention.

Among highly proliferating tissues, only the small intestines showed a significant uptake of [^{18}F]NFT202. However, over 70% of the radioactivity was distributed in the content, with only the remaining 30% trapped in the tissues (data not shown). This observation showed that [^{18}F]NFT202 or its metabolite was excreted through the liver into the intestine and/or was actively transported from the basal side to the apical side through the intestinal epithelial cell membrane. From another point of view, even in the most highly proliferating tissues in rodents, [^{18}F]NFT202 was not effectively trapped.

Considering these results, we concluded that [^{18}F]NFT202 is not a suitable PET ligand for imaging tumor cell proliferation. Consistent with previous validation studies [1], our results also suggested that, in order to predict in vivo performance of nucleoside derivatives, we should consider the detailed cellular and molecular biochemistry of nucleoside metabolism.

Acknowledgments

We thank Mr. Kenji Frutuka for his excellent assistance with MS analysis.

References

[1] Grierson JR, Schwartz JL, Muzi M, Jordan R, Krohn KA. Metabolism of 3′-deoxy-3′-[F-18]fluorothymidine in proliferating A549 cells: validations for positron emission tomography. Nucl Med Biol 2004; 31:829–37.

[2] Martin SJ, Eisenbarth JA, Wagner-Utermann U, Mier W, Henze M, Pritzkow H, et al. A new precursor for the radiosynthesis of [^{18}F]FLT. Nucl Med Biol 2002;29:263–73.

[3] Edgell WF, Parts L. Synthesis of alkyl and substituted alkyl fluorides from *p*-toluenesulfonic acid esters. The preparation of *p*-toluenesulfonic acid esters of lower alcohols. J Am Chem Soc 1955;77:4899–902.

[4] Kit S, Dubbes DR, Piekarski LJ, Hsu TC. Deletion of thymidine kinase activity from L cells resistant to bromodeoxyuridine. Exp Cell Res 1963;31:297–312.

[5] Ayusawa D, Shimizu K, Koyama H, Kaneda S, Takeishi K, Seno T. Cell-cycle-directed regulation of thymidylate synthase messenger RNA in human diploid fibroblasts stimulated to proliferate. J Mol Biol 1986;190:559–67.

[6] Chi DY, Kilbourn MR, Katzenellenbogen JA, Brodack JW, Welch MJ. Synthesis of no-carrier-added *N*-([^{18}F]fluoroalkyl)spiperone derivatives. Appl Radiat Isot 1986;37:1173–80.

[7] Hamacher K, Coenen HH, Stocklin G. Efficient stereospecific synthesis of no-carrier-added 2-[^{18}F]-fluoro-2-deoxy-D-glucose using aminopolyether supported nucleophilic substitution. J Nucl Med 1986;27: 235–8.

[8] Toyohara J, Waki A, Takamatsu S, Yonekura Y, Magata Y, Fujibayashi Y. Basis of FLT as a cell proliferation marker: comparative uptake studies with [^{3}H]thymidine and [^{3}H]arabinothymidine, and cell-analysis in 22 asynchronously growing tumor cell lines. Nucl Med Biol 2002;29:281–7.

[9] Mori T, Kasamatsu S, Mosdzianowski C, Welch MJ, Yonekura Y, Fujibayashi Y. Automatic synthesis of 16α-[^{18}F]fluoro-17β-estradiol ([^{18}F]FES) using a cassette-type [^{18}F]fluorodeoxyglucose synthesizer. Nucl Med Biol 2006;33:281–6.

[10] van Waarde A, Cobben DC, Suurmeijer AJ, Maas B, Vaalburg W, de Vries EF, et al. Selectivity of ^{18}F-FLT and ^{18}F-FDG for differentiating tumor from inflammation in a rodent model. J Nucl Med 2004;45: 695–700.

[11] Rasey JS, Grierson JR, Wiens LW, Kolb PD, Schwartz JL. Validation of FLT uptake as a measure of thymidine kinase-1 activity in A549 carcinoma cells. J Nucl Med 2002;43:1210–7.

[12] Guo Y, Kotova E, Chen Z-S, Lee K, Hopper-Borge E, Belinsky MG, et al. MRP8, ATP-binding cassette C11 (ABCC11), is a cyclic nucleotide efflux pump and a resistance factor for fluoropyrimidines 2′,3′-dideoxycytidine and 9′-(2′-phosphonylmethoxyethyl)adenine. J Biol Chem 2003;278:29509–14.

[13] Barthel H, Cleij MC, Collingridge DR, Hutchinson OC, Osman S, He Q, et al. 3′-Deoxy-3′-[^{18}F]fluorothymidine as a new marker for monitoring tumor response to antiproliferative therapy in vivo with positron emission tomography. Cancer Res 2003;63:3791–8.

[14] Barthel H, Perumal M, Latigo J, He Q, Brady F, Luthra SK, et al. The uptake of 3′-deoxy-3′-[^{18}F]fluorothymidine into L5178Y tumors in vivo is dependent on thymidine kinase 1 protein levels. Eur J Nucl Med Mol Imaging 2005;32:257–63.

資料(11)

Available online at www.sciencedirect.com
ScienceDirect
Nuclear Medicine and Biology 34 (2007) 205–210
NUCLEAR MEDICINE — AND — BIOLOGY
www.elsevier.com/locate/nucmedbio

In vivo imaging of estrogen receptor concentration in the endometrium and myometrium using FES PET — influence of menstrual cycle and endogenous estrogen level

Tatsuro Tsuchida[a,*], Hidehiko Okazawa[b], Tetsuya Mori[b], Masato Kobayashi[b], Yoshio Yoshida[c], Yasuhisa Fujibayashi[b], Harumi Itoh[a]

[a]*Department of Radiology, Faculty of Medical Sciences, University of Fukui, Yoshida-gun, Fukui 910-1193, Japan*
[b]*Biomedical Imaging Research Center, University of Fukui, Yoshida-gun, Fukui 910-1193, Japan*
[c]*Department of Obstetrics and Gynecology, Faculty of Medical Sciences, University of Fukui, Yoshida-gun, Fukui 910-1193, Japan*

Received 17 October 2006; received in revised form 5 December 2006; accepted 13 December 2006

Abstract

Purpose: The goals of this study were to measure estrogen receptor (ER) concentration in the endometrium and myometrium using 16α-[^{18}F]fluoro-17β-estradiol (FES) positron emission tomography (PET) and to investigate the relationship between changes in these parameters with the menstrual cycle and endogenous estrogen levels.

Methods: Sixteen female healthy volunteers were included in this study. After blood sampling to measure endogenous estrogen level, FES PET image was acquired 60 min postinjection of FES. After whole-body imaging of FES PET, averaged standardized uptake values (SUVs) in the endometrium and myometrium were measured, and the relationship between FES uptake and menstrual cycle or endogenous estrogen level was evaluated.

Results: Endometrial SUV was significantly higher in the proliferative phase than in the secretory phase (6.03±1.05 vs. 3.97±1.29, P=.022). In contrast, there was no significant difference in myometrial SUV when the proliferative and secretory phases were compared (P=.23). Further, there was no correlation between SUV and endogenous estrogen level in the proliferative phase.

Conclusions: The change of ER concentration relative to menstrual cycle as characterized by FES PET was consistent with those from previous reports that used an immunohistochemical technique. These data suggest that FES PET is a feasible, noninvasive method for characterizing changes in ER concentration.

Keywords: Estrogen receptor concentration; 16α-[^{18}F]fluoro-17β-estradiol (FES); Positron emission tomography (PET); Menstrual cycle; Endogenous estrogen level

1. Introduction

16α-[^{18}F]fluoro-17β-estradiol (FES) is a radiopharmaceutical that binds to the estrogen receptor (ER) and expresses the existence of ER [1]. FES can help characterize the diagnosis and efficacy of hormonal therapy in patients with ER-positive breast cancer [2–6]. Indeed, Mintun et al. [2] reported that in vivo uptake of FES in primary breast carcinoma correlates with in vitro measurements of ER concentration and thereby represents a noninvasive quantitative measurement of ER in breast carcinoma. Although several studies reported the expression of ER in many organs other than breast using immunohistochemistry [7], such findings are yet to be confirmed in human studies, even in normal ER-rich tissue like the endometrium or myometrium. Because FES is expected to be a good tracer to reveal the change of ER concentration in normal tissue as well as in disease, normal control data should be required. In immunohistochemical studies, the relationships between the level of ER and menstrual cycle in the endometrium and myometrium are reported as follows [8–17]. In the endometrium, the level of ER increases from the early to the late proliferative phase and decreases in the secretory phase. In the myometrium, the cyclical change of ER varies

* Corresponding author. Tel.: +81 776 61 3111x2335; fax: +81 776 61 8137.
E-mail address: tsucchy@fmsrsa.fukui-med.ac.jp (T. Tsuchida).

0969-8051/$ – see front matter © 2007 Published by Elsevier Inc.
doi:10.1016/j.nucmedbio.2006.12.003

Fig. 1. Sagittal PET image of FES distribution in a healthy woman (left) and representative ROIs placed on the endometrium (open circles) and myometrium (dotted circles) (right). Image was acquired 60 min postinjection of 185 MBq of FES.

in different layers. The inner part of the myometrium (stratum subvasculare) adjacent to the endometrium shows the same behavior as the endometrium does. On the other hand, the outer part of the myometrium (stratum vasculare and supravasculare) shows the constant ER expression through the entire menstrual cycle. It is well known that the endogenous estrogen level alters during menstrual cycle, which has two peaks in the late proliferative and mid-secretory phase, and thus, the effect of estrogen level on FES uptake should also be studied before clinical application. Therefore, the goals of this study were to measure ER concentration in the endometrium and myometrium using FES positron emission tomography (PET) and to investigate the relationship between changes in these parameters with the menstrual cycle and the endogenous estrogen level in healthy volunteers.

2. Materials and methods

2.1. Subjects

Sixteen female normal volunteers were included in this study. Participants' age ranged from 21 to 28 years old (23.6±2.2 years; mean±S.D.). Medical interviews, which encompass previous malignancy and gynecological surgery, menstrual state and cycle and the last menstrual period, were conducted in all subjects. Written informed consent was obtained from all subjects participating in this study, which was approved by the Institutional Review Board of University of Fukui Hospital.

2.2. Synthesis of FES

FES synthesis was performed according to the method of Kiesewetter et al. [1], with modifications as reported by Mori et al. [18] in detail. A cassette-type automatic [^{18}F]fluorodeoxyglucose (FDG) synthesizer (TRACERlab MXFDG, GE Medical Systems, Milwaukee, WI) that was modified for the synthesis of FES was utilized, and fluorination, two-step hydrolysis and neutralization were performed under the appropriate condition to synthesize FES. After the final purification, the radiochemical purity

Table 1
Characteristics of the subjects and summary of the results

Phase	Age (years)	Number of days from the onset of menses	E2 (pg/ml)	SUV in the endometrium	SUV in the myometrium
Menstrual phase	21	2	33	5.77	2.62
	25	4	33	4.81	2.67
Proliferative phase	27	8	71	5.73	2.55
	22	10	51	6.5	2.64
	23	11	45	4.68	2.5
	22	13	46	5.6	2.82
	21	13	83	7.81	3
	24	14	60	5.87	2.98
			Mean±S.D.	6.03±1.05	2.75±0.22
Secretory phase	25	19	186	4.19	3.16
	25	21	112	2.87	2.54
	22	23	154	2.9	2.3
	22	24	58	5.95	2.64
	24	26	72	3.16	1.94
	21	26	39	5.51	2.6
	28	27	48	3.2	2.53
			Mean±S.D.	3.97±1.29	2.53±0.37
Irregular	26	32	51	3.31	2.55

was greater than 99%, and the yield was 42.4±3.2% (EOB). The specific activity calculated by the analytical HPLC system was more than 111 GBq/μmol.

2.3. PET imaging

All subjects fasted more than 4 h prior to FES PET examination to eliminate the excretion of FES from the hepatobiliary system and the gastrointestinal tract, which would otherwise interfere with image interpretation in the pelvic space. Three milliliters of blood was obtained just before FES injection to measure the endogenous estrogen level [estradiol (E2)]. FES PET data acquisition started 60 min after the injection of 185 MBq of FES. Emission scans were performed for 3 min in the pelvic portion (two bed positions) and for 2 min in the remaining positions (five bed positions) to cover the area from the head to the inguinal region. Postinjection transmission scans for 2 min at the pelvis and for 1 min in other parts were performed after the emission scans for attenuation correction. The acquired data were reconstructed using an iterative reconstruction method with 14 subsets and two iterations. The reconstructed image was converted to standardized uptake value (SUV) image according to the subject's body weight and net injected dose for the data analysis.

2.4. Magnetic resonance imaging

All subjects underwent MRI examination on the same day FES PET was performed or 1 day before FES PET was carried out to obtain positional information regarding the endometrium and myometrium. T_1- and T_2-weighted images (WIs) in the transaxial plane and T_2-WI in the sagittal plane were acquired using a 1.5-T superconducting MRI system (Signa, GE Medical Systems). The imaging sequence of T_1-WI and T_2-WI was 533/8 and 4700/90 ms (TR/TE), respectively.

2.5. Data analysis

On the midsagittal image of FES PET, circular regions of interest (ROIs: 8 mm in diameter) were placed using guidance by T_2-WI of MRI in the sagittal plane. By comparing FES PET and MRI visually, the endometrium, which usually has high uptake of FES compared with the myometrium, was identified. The myometrium was defined as the faint FES uptake area surrounding the endometrium. Three ROIs were placed on the endometrium and nine were placed on the myometrium, as shown in Fig. 1. The averaged SUVs in the endometrium and myometrium were plotted against the number of days from the onset of menses and the endogenous estrogen level.

In this study, the menstrual cycle was classified into two groups because of the limited number of subjects: (1) the proliferative phase (6 to 14 days after the onset of menses) and (2) the secretory phase (15 to 28 days from the onset of menses). SUVs between these two phases were compared in the endometrium and myometrium. Nonparametric Mann–Whitney U test was used for statistical comparisons. Spearman nonparametric correlation analysis was performed to analyze the relationship between SUVs in both the endometrium and the myometrium and E2. In each statistical analysis, $P<.05$ was considered to represent statistical significance.

3. Results

Characteristics of the subjects and a summary of the results are shown in Table 1.

One subject had an irregular menstrual cycle and was excluded from the analysis regarding the relationship between FES uptake and menstrual cycle. Based on the menstrual cycle classification mentioned in the Data analysis section, six subjects were classified as being in the proliferative phase and seven were classified as being in

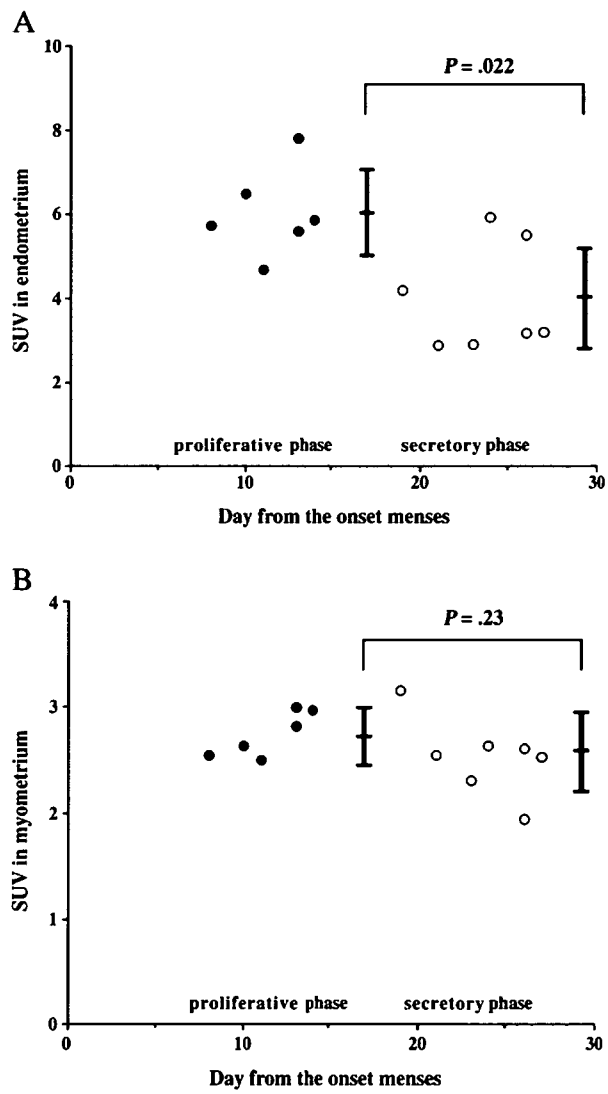

Fig. 2. Changes in FES uptake in the uterus during the menstrual cycle. Endometrial FES uptake (A) was significantly higher in the proliferative phase (filled circle) than in the secretory phase (open circle). By contrast, myometrial FES uptake (B) was similar when the two phases are compared.

the secretory phase. Two subjects were in the menstrual phase and were also excluded from this analysis. In the analysis of the relationship between FES uptake and E2 level, no subjects were excluded.

Fig. 2A shows the relationship between endometrial SUV and the menstrual cycle. SUV was significantly higher in the proliferative phase than in the secretory phase (6.03±1.05 vs. 3.97±1.29, P=.022).

The relationship between myometrial SUV and the menstrual cycle is illustrated in Fig. 2B. No significant difference in SUV was noted when the proliferative and secretory phases were compared (2.75±0.22 vs. 2.53±0.37, P=.23).

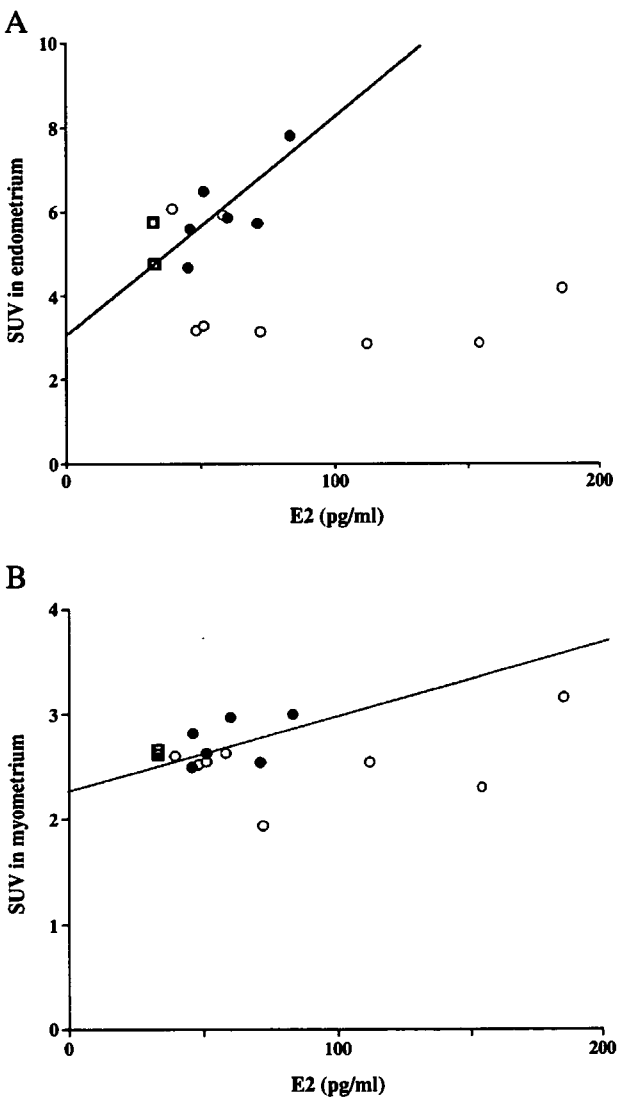

Fig. 3. Relationship between FES uptake and endogenous estrogen level. Linear regression analysis (solid line) was performed only in the proliferative phase (filled circle). No significant linear correlation was observed in the endometrium (A) (y=0.05x+2.95, r^2=.56, P=.09) or the myometrium (B) (y=0.006x+2.37, r^2=.20, P=.38). Open circles represent SUV in the proliferative phase, and open squares represent SUV in the menstrual phase.

Further, there was no relationship between FES uptake and E2 level in the endometrium (Fig. 3A) or myometrium (Fig. 3B) in the proliferative phase.

4. Discussion

Physiological FES uptake in the endometrium is affected by the menstrual cycle secondary to changes in endogenous estrogen level in healthy women. However, the present study demonstrated that endometrial SUV was not directly correlated with plasma E2 level or FES uptake in the myometrium. Yoo et al. [19] reported that FES preferentially binds the ERα subtype with 6.3-fold higher affinity than that for ERβ. Further, the uterus is one of the target organs of E2 and expresses both ERα and ERβ. ERα predominates in the uterus, breast, kidney, liver and heart, whereas tissues that have high ERβ levels include those of the prostate, testes, ovaries, gastrointestinal tract, lung, bladder and hematopoietic and central nervous systems. Many tissues contain both ERα and ERβ, such as breast, epididymis, thyroid, adrenal and bone tissues. Wang et al. [20] used immunohistochemistry to demonstrate that the myometrium and leiomyomas have ERα-dominant expression. These results suggested that uterine ER expression is a good target for study with FES PET. However, physiological FES uptake in the uterus of healthy women remains unclear and may vary with the menstrual cycle observed in FDG PET [21].

Several investigators have used immunohistochemistry to characterize the relationship between ER expression and menstrual cycle measured in the endometrium [8–17] and myometrium [9–16]. In these reports, endometrial ER concentration in the proliferative phase was higher than that in the secretory phase, which is consistent with results from the present study. Further, several studies have reported a significant difference between myometrial ER concentration in the proliferative and secretory phases. By contrast, the present study showed no significant difference in myometrial FES uptake when the proliferative and secretory phases were compared. This finding is supported by some papers [14–16]. Noe et al. [15] and Vienonen et al. [16] reported that in the myometrium, ERα was regulated in the layer adjacent to the endometrium in an endometrium-like pattern during the menstrual cycle, whereas expression pattern in the outer part of the myometrium was more stable. In the studies that showed a significant difference between myometrial ER concentration in the proliferative and secretory phases, only the myometrium immediately underlying the endometrium was analyzed as the representative of the whole uterine muscular wall [9–11]. In the present study, ROIs that were placed on the myometrium, which surrounded endometrial ROIs, evaluated the outer part of the myometrium because of the limited spatial resolution.

In this study, there was no significant relationship between FES uptake and E2 even in the proliferative phase. A previous study reported that a large concentration of endometrial ER in

the late proliferative phase correlates with the plasma E2 surge [22]. Further, Levy et al. [8] reported that a significant correlation was observed between ER concentration and E2 in the proliferative phase. In the present study, there was a trend toward a relationship between E2 and SUV in the endometrium in the proliferative phase (P=.09), but the difference did not reach the level of statistical significance. Repetition of the present study with a large population size may result in data consistent with those reported by Levy et al.

The relationship between ER concentration in the myometrium and endogenous estrogen level demonstrated no statistical significance. FES uptake in the myometrium was almost constant throughout the entire menstrual cycle and may be independent from the change of endogenous estrogen level in healthy volunteers.

Although FES represents the level of unoccupied ER and ER measured with immunohistochemistry represents total ER, our results and the previous reports showed the same behavior. Katzenellenbogen et al. [23] reported that the FES uptake in the uterus was suppressed by the coinjection of a high dose of E2 or the tamoxifen pretreatment in the rat. However, although total ER and occupied ER by endogenous estrogen in the endometrium will increase in the proliferative phase, the proportion of unoccupied ER measured with FES will not change. In the secretory phase, the opposite phenomenon will occur and the proportion of unoccupied ER will not change as well. Therefore, it is speculated that the behavior of total ER and unoccupied ER will be similar. In the myometrium, total and unoccupied ER in the proliferative phase did not change when the endogenous estrogen increased. The proportion of occupied ER against total ER may be small enough, although further examination will be required.

FES has been used for the evaluation of breast tumors [2–6] and may also have a clinical application in patients with uterine endometrium-related gynecological diseases [24,25]. Indeed, Okazawa et al. [25] reported that the combination of FDG PET and FES PET improved the diagnostic accuracy in various uterine endometrium-related gynecological diseases including uterine endometrial cancer, adenomyosis and endometrial hyperplasia. For the assessment of FES uptake, SUV or lesion-to-normal ratio will be feasible. The present study demonstrated that FES uptake in the endometrium varied with the menstrual cycle, whereas myometrial FES uptake was stable throughout the entire menstrual cycle. These data suggest that the myometrium may serve as a good internal control during FES studies of other organ systems and that the menstrual cycle should be taken account of when the endometrium was considered for an internal control.

5. Conclusion

The change of ER concentration relative to menstrual cycle as characterized by FES was consistent with those from previous reports that used an immunohistochemical technique. Further, these data suggest that FES PET is a feasible, noninvasive method for characterizing changes in ER concentration.

Acknowledgments

The authors thank Miyuki Tamaru, Mika Ito and other staff members of the Biological Imaging Research Center, University of Fukui, for technical and clinical support. This study was partly funded by the Research and Development Project Aimed at Economic Revitalization (Leading Project) from MEXT Japan and by the 21st Century COE Program (Medical Science) from the Japan Society for the Promotion of Science.

References

[1] Kiesewetter DO, Kilbourn MR, Landvatter SW, Heiman DF, Katzenellenbogen JA, Welch MJ. Preparation of four fluorine-18-labeled estrogen and their selective uptake in target tissue of immature rats. J Nucl Med 1984;25:1212–21.
[2] Mintun MA, Welch MJ, Siegel BA, Mathias CJ, Brodack JW, McGuire AH, et al. Breast cancer: PET imaging of estrogen receptors. Radiology 1988;169:45–8.
[3] McGuire AH, Dehdashti F, Siegel BA, Lyss AP, Brodack JW, Mathias CJ, et al. Positron tomographic assessment of 16α-[^{18}F]fluoro-17β-estradiol uptake in metastatic breast carcinoma. J Nucl Med 1991;32:1526–31.
[4] Dehdashti F, Mortimer JE, Siegel BA, Griffeth LK, Bonasera TJ, Fusselman MJ, et al. Positron tomographic assessment of estrogen receptors in breast cancer: comparison with FDG-PET and in vitro receptor assays. J Nucl Med 1995;36:1766–74.
[5] Dehdashti F, Flanagan FL, Mortimer JE, Katzenellenbogen JA, Welch MJ, Siegel MA. Positron emission tomographic assessment of "metabolic flare" to predict response of metastatic breast cancer to antiestrogen therapy. Eur J Nucl Med 1999;26:51–6.
[6] Mortimer JE, Dehdashti F, Siegel BA, Trinkaus K, Katzenellenbogen JA, Welch MJ. Metabolic flare: indicator of hormone responsiveness in advanced breast cancer. J Clin Oncol 2001;19:2797–803.
[7] Nilsson S, Makela S, Treuter E, Tujague M, Thomsen J, Andersson G, et al. Mechanisms of estrogen action. Physiol Rev 2001;81:1535–65.
[8] Levy C, Robel P, Gautray JP, De Brux J, Verma U, Descomps B, et al. Estradiol and progesterone receptors in human endometrium: normal and abnormal menstrual cycle and early pregnancy. Am J Obstet Gynecol 1980;136:646–51.
[9] Lessey BA, Killan AP, Metzger A, Haney AF, Greene GL, McCarty KS. Immunohistochemical analysis of human uterine estrogen and progesterone receptors throughout the menstrual cycle. J Clin Endocrinol Metab 1988;67:334–40.
[10] Kawaguchi K, Fujii S, Konishi I, Iwai T, Nanbu Y, Nonogaki H, et al. Immunohistochemical analysis of oestrogen receptors, progesterone receptors and Ki-67 in leiomyoma and myometrium during menstrual cycle and pregnancy. Virchows Arch A Pathol Anat 1991;419:309–15.
[11] Snijders MPML, de George AFPM, Cetets-Te Baerts MJC, Rousch MJM, Koudstaal J, Bosman FT. Immunocytochemical analysis of oestrogen receptors and progesterone receptors in human uterus throughout the menstrual cycle and after the menopause. J Reprod Fertil 1992;94:363–71.
[12] Englund K, Blanck A, Gustavsson I, Lundkvist U, Sjöblom P, Norgren A, et al. Sex steroid receptors in human myometrium and fibrosis: changes during the menstrual cycle and gonadotropin-

releasing hormone treatment. J Clin Endocrinol Metab 1998;83: 4092–6.

[13] Mertens HJMM, Heineman MJ, Theunissen PHMH, de Jong FH, Evers JLH. Androgen, estrogen and progesterone receptor expression in the human uterus during menstrual cycle. Eur J Obstet Gynecol Reprod Biol 2001;98:58–65.

[14] Nisolle M, Gillerot S, Casanas-Roux F, Squifflet J, Berliere M, Donnez J. Immunohistochemical study of the proliferation index, oestrogen receptors and progesterone receptors A and B in leiomyoma and normal myometrium during menstrual cycle and under gonadotropin-releasing hormone agonist therapy. Hum Reprod 1999;14:2844–50.

[15] Noe M, Kunz G, Herbertz M, Mall G, Leyendecker G. The cyclic pattern of the immunocytochemical expression of oestrogen and progesterone receptors in human myometrial and endometrial layers: characterization of the endometrial–subendometrial unit. Hum Reprod 1999;14:190–7.

[16] Vienonen A, Miettinen S, Bläuer M, Martikainen PM, Tomás E, Heinonen PK, et al. Expression of nuclear receptors and cofactors in human endometrium and myometrium. J Soc Gynecol Investig 2004;11:104–12.

[17] Shiozawa T, Shih H, Miyamoto T, Feng Y-Z, Uchikawa J, Itoh K, et al. Cyclic changes in the expression of steroid receptor coactivators and corepressors in the normal human endometrium. J Clin Endocrinol Metab 2003;88:871–8.

[18] Mori T, Kasamatsu S, Mosdzianowski C, Welch MJ, Yonelura Y, Fujibayashi Y. Automatic synthesis of 16α-[^{18}F]fluoro-17β-estradiol using a cassette-type [^{18}F] fluorodeoxyglucose synthesizer. Nucl Med Biol 2006;33:281–6.

[19] Yoo J, Dence CS, Sharp TL, Katzenellenbogen JA, Welch MJ. Synthesis of an estrogen receptor β-selective radioligand: 5-[^{18}F]fluoro-(2*R**,3*S**)-2,3-bis (4-hydroxyphehyl)pentanenitrile and comparison of in vivo distribution with 16α-[^{18}F]fluoro-17β-estradiol. J Med Chem 2005;48:6366–78.

[20] Wang H, Wu X, Englund K, Masironi B, Eriksson H, Sahlin L. Different expression of estrogen receptors alpha and beta in human myometrium and leiomyoma during the proliferative phase of the menstrual cycle and after GnRHa treatment. Gynecol Endocrinol 2001;15:443–52.

[21] Nishizawa S, Inubushi M, Okada H. Physiological ^{18}F-FDG uptake in the ovaries and uterus of healthy female volunteers. Eur J Nucl Med Mol Imaging 2005;32:549–56.

[22] Robertson DM, Mester J, Beilby J, Steele SJ, Kellie AF. The measurement of high-affinity oestradiol receptors inhuman uterine endometrium and myometrium. Acta Endocrinol 1971;68:534–42.

[23] Katzenellenbogen JA, Mathias CJ, Vanbrocklin HF, Brodack JW, Welch MJ. Titration of the in vivo uptake of 16α-[^{18}F]fluoroestradiol by target tissues in the rat: comparison by tamoxifen, and implications for quantitating estrogen receptors in vivo and the use of animal models in receptor-binding radiopharmaceutical development. Nucl Med Biol 1993;20:735–45.

[24] Yoshida Y, Kurokawa T, Yagihara R, Kotsuji F. The usefulness of FES-PET for the prediction of the therapeutic effect of hormonal therapy in a patient with endometrial cancer — a case report (abstract). J Obstet Gynaecol Res 2006;58:406.

[25] Okazawa H, Yoshida Y, Mori T, Tsuchida T, Kurokawa T, Kobayashi M, et al. Evaluation of uterine endometrium related gynecological diseases using F-18 fluoroestradiol and PET (Abstract). J Nucl Med 2006;47:318.

資料(12)

Available online at www.sciencedirect.com
ScienceDirect
Gynecologic Oncology 104 (2007) 764–766
Gynecologic Oncology
www.elsevier.com/locate/ygyno

Case Report

The positron emission tomography with F18 17β-estradiol has the potential to benefit diagnosis and treatment of endometrial cancer

Yoshio Yoshida [a,*], Tetsuji Kurokawa [a], Yoko Sawamura [a], Akiko Shinagawa [a], Hidehiko Okazawa [b], Yasuhisa Fujibayashi [b], Fumikazu Kotsuji [a]

[a] *Department of Obstetrics and Gynecology, Faculty of Medical Sciences, University of Fukui, Matsuoka-cho, Yoshida-gun, Fukui-ken 910-1193, Japan*
[b] *Biomedical Imaging Research Center, Faculty of Medical Sciences, University of Fukui, Matsuoka-cho, Yoshida-gun, Fukui-ken 910-1193, Japan*

Received 18 July 2006
Available online 6 December 2006

Abstract

Background. The positron emission tomography (PET) with F18 17β-estradiol (FES) has good imaging for assessment of estrogen receptor in breast cancer.

Case. We report on a 30-year-old woman who desired to preserve her fertility with well-differentiated endometrial adenocarcinoma. Before hormone treatment was started, FES-PET showed increased uptake of endometrium, magnetic resonance imaging (MRI) showed thickness and F-18 fluorodeoxyglucose (FDG)-PET showed increased uptake. FES-PET after 3 months showed remaining FES uptake, but there were no abnormal findings on MRI and FDG-PET. Hysteroscopy showed remaining adenocarcinoma. After additional treatment, FES-PET showed a therapeutic response, and hysteroscopy showed no abnormal finding.

Conclusions. To our knowledge, this is the first report that FES-PET has the potential to provide more useful information than did FDG-PET about the hormone therapy.

Keywords: FES-PET; Endometrial cancer; Endocrine treatment

Introduction

Endometrial cancer is the most common gynecological malignancy in North American and European women, and the incidence continues to rise. Mortality from endometrial cancer ranks eighth among cancer deaths in North American women, and in Europe nearly 10,000 women die of this disease each year [1]. For young women (under age 40) who desired to preserve their fertility with well-differentiated endometrial adenocarcinoma, conservative treatment with periodic use of progestin is available [2,3]. Present methods to assess tumor responsiveness require a tissue sample obtained by performing a dilatation and curettage (D & C) every 3 months [3]. Sample availability is thus limited by potential morbidity and sampling problems. A noninvasive method to assess tumor responsiveness would avoid unnecessary diagnostic biopsies of the endometrium and permit serial assessments during treatment.

Positron emission tomography (PET) is a highly sensitive, noninvasive technology that is ideally suited for pre-clinical and clinical imaging of cancer biology, in contrast to anatomical approaches. By using radiolabeled tracers, PET can yield cross-sectional images that reflect tissue biochemistry [4]. Two radiolabeled tracers hold promise for the diagnosis and management of endometrial cancer. The most extensively studied of these is F-18 fluorodeoxyglucose (FDG); the other one is F-18 17β-estradiol (FES) [4]. FES-PET has good imaging characteristics in human studies to predict response to endocrine treatment in breast cancer [5]. But there has been no report published on whether FES-PET provides information useful for assessing tumor response to systemic therapy, or whether FES-PET provides more useful information than FDG-PET in endometrial cancer.

Case

We report on an unmarried 30-year-old woman who presented with well-differentiated adenocarcinoma (Fig. 1A)

* Corresponding author. Fax: +81 776 61 8117.
E-mail address: yyoshida@fmsrsa.fukui-med.ac.jp (Y. Yoshida).

0090-8258/$ - see front matter © 2006 Elsevier Inc. All rights reserved.
doi:10.1016/j.ygyno.2006.10.024

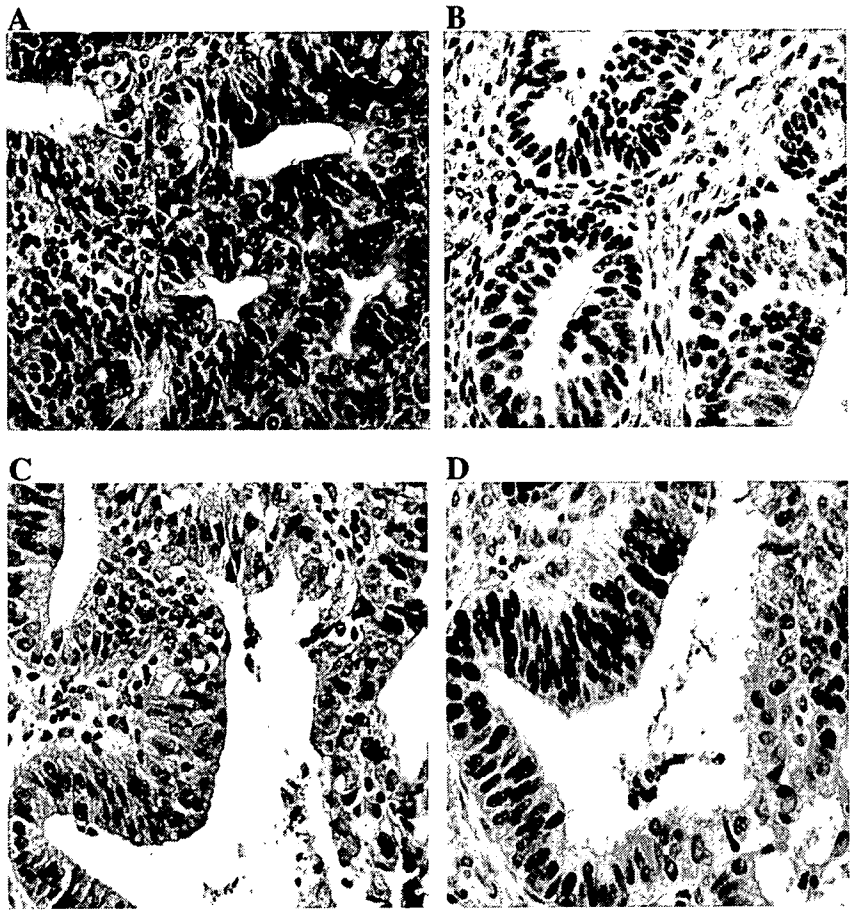

Fig. 1. Histopathology examination of curettaged tissue of endometrium. First curetttaged tissue: (A) hematoxylin and eosin staining showing well-differentiated endometrial adenocarcinoma (magnification ×400), (B) strong positive immunostaining for estrogen receptor (magnification ×400). Second curetttaged tissue: (A) hematoxylin and eosin staining showing remaining focal well-differentiated endometrial adenocarcinoma (magnification ×400), (B) moderate positive immunostaining for estrogen receptor (magnification ×400).

that an endometrial biopsy showed was predominantly estrogen receptor (ER) positive (Fig. 1B). She had a history of polycystic ovary and had received sequential hormone replacement therapy (HRT). Because she desired to preserve her fertility, medical treatment was desirable. In a recent review of women under age 40 with well-differentiated adenocarcinoma, conservative treatment with periodic use of progestin was used [2], and informed consent was obtained from a patient. Before

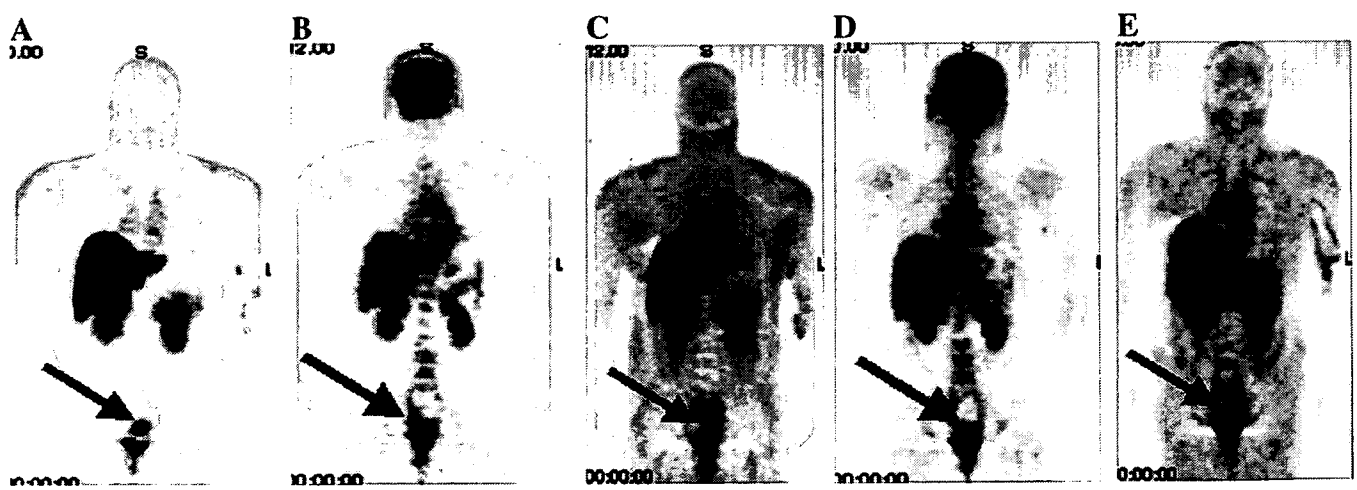

Fig. 2. Endometrial PET during hormonal treatment. Before initiation of treatment: (A) FES-PET showed clearly increased uptake in the endometrium regions and (D) FDG-PET showed slightly increased uptake equivalent to liver uptake. Three months after initiation of treatment, FES-PET showed (B) remaining FES uptake in endometrium site, but (E) FDG-PET showed no abnormal finding. After additional treatment, (C) FES-PET showed no abnormal findings.

progestin treatment was started in our patient, FES-PET showed clearly increased uptake in the endometrium regions; the maximum standardized uptake value (SUV) was 12.5 (Fig. 2A) at late pseudo-secretory phase (day 3 before withdraw bleeding), magnetic resonance imaging (MRI) showed slight thickness of endometrium and FDG-PET showed slightly increased uptake equivalent to liver uptake (Fig. 2B). First, the patient was treated with medroxyprogesterone acetate (MPA) 200 mg per day [6,7]. FES-PET after 3 months showed remaining FES uptake in endometrium site (SUV 6.3) (Fig. 2C), but there were no abnormal findings on MRI and FDG-PET (Fig. 2D). Hysteroscopy and endometrial curettage specimens showed remaining focal well-differentiated adenocarcinoma (Fig. 1C) with moderate ER positivity (Fig. 1D). Next, she was treated with MPA 600 mg per day [6,7]. After more than 3 months, FES-PET showed a therapeutic response (Fig. 2E), and there were no abnormal findings on hysteroscopy and endometrial curettage specimens.

Discussion

To our knowledge, this is the first report showing that FES-PET has the potential to provide functional information about the hormone responsiveness of well-differentiated endometrial adenocarcinoma. When we performed serial FES-PET imaging in a woman with well-differentiated adenocarcinoma treated with MPA, a decrease in FES-PET uptake was seen after a therapeutic response. This decrease correlated with the pathological evaluation. Although the pathological evaluation is the "golden" criteria, FES-PET is a new way to evaluate ER activity in endometrial adenocarcinoma.

The standard method of assessing uterine neoplasms is the formal fractional D & C. But to provide sufficient diagnostic information this method requires that patients are anesthetized [3]. At present, FDG-PET is not incorporated in routine clinical practice for diagnosis of gynecologic cancer or assessment of tumor responsiveness to treatment. However, current clinical applications of FDG in gynecologic cancer diagnosis and management have shown many benefits [8]. On the other hand, the limitation of FDG-PET has been shown to provide lower diagnostic accuracy in detecting minimal lesions as well as some pre-forms of cancer and showing no specificity for cancer detection in general. FDG activity can be seen in the gastrointestinal tract, bladder and inflammatory lesions [8,9].

More than 80% of endometrial cancers are usually associated with a history of unopposed estrogen exposure or other hyperestrogenic risk factors such as obesity [1]. And, it has been well documented that the ER level usually is extremely high especially in well-differentiated endometrial adenocarcinoma. An increased response rate to hormonal agents, including progestin, has been associated with positive estrogen or progesterone receptor status. The PR is a product resulting from estrogen binding to the ER. In some studies, the PR appears to be a better predictor of hormone responsiveness than the ER [2]. Yet, the question is whether FES uptake predicts hormone responsiveness more accurately than does the PR. In this case, FES-PET provided functional information about hormone responsiveness in well-differentiated endometrial adenocarcinoma, similar to that of estrogen dependency of breast cancer.

It is important to take into consideration the cyclic changes in estradiol and estrogen receptor when the potential role of FES-PET in premenopausal women is evaluated because estradiol increases and progesterone decreases ER expression. In this case, FES-PET was performed at late pseudo-secretory phase (day 3 before withdraw bleeding) and showed clearly increased uptake in the endometrium regions. During the physiological cycle or during HRT, ER levels are lower in the secretory phase than in other phases of the cycle [10]. Thus, FES-PET has the potential to provide functional information about ER activity in well-differentiated endometrial adenocarcinoma.

In summary, FES-PET showed increased uptake of FES in well-differentiated endometrial adenocarcinoma and provided information for assessing tumor response to hormonal therapy; FES-PET provided more useful information than did FDG-PET. These observations highlight the need for further systemic studies on the utility of FES-PET in gynecologic cancer.

References

[1] Amant F, Neven P, Timmerman D, Van Limbergen E, Vergote I. Endometrial cancer. Lancet 2005;366:491–505.
[2] Curtin JP, Kavanagh JJ, Fox H, Spanos Jr WJ, Corpus. Mesenchymal tumors. In: William JH, Carlos AP, Robert CY, editors. Principles and Practice of Gynecologic Oncology. 3rd ed. Philadelphia: Lippincott Williams & Wilkins; 1999. p. 961–79.
[3] Pecorelli S, Fallo L, Sartori E, Gastaldi A. Preinvasive lesions of the endometrium. Ann N Y Acad Sci 1991;622:449–62.
[4] Gambhir SS. Molecular imaging of cancer with positron emission tomography. Nat Rev, Cancer 2002;2:683–93.
[5] Linden HM, Stekhova SA, Link JM, Gralow JR, Livingston RB, Ellis GK, et al. Quantitative fluoroestradiol positron emission tomography imaging predicts response to endocrine treatment in breast cancer. J Clin Oncol 2006;24:2793–9.
[6] Randall TC, Kurman RJ. Progestin treatment of atypical hyperplasia and well-differentiated carcinoma of the endometrium in women under age 40. Obstet Gynecol 1997;90:434–40.
[7] Podratz KCO, Brien PC, Malkasian GD, Decker Jr DG, Jefferies JA. Effects of progestational agents in treatment of endometrial carcinoma. Obstet Gynecol 1985;66:106–10.
[8] Kumar R, Alavi A. PET imaging in gynecologic malignancies. Radiol Clin North Am 2004;42:1155–67.
[9] Lerman H, Metser U, Grisaru D, Fishman A, Kievshitz G, Even-Sapir E. Normal and abnormal 18F-FDG endometrial and ovarian uptake in pre- and postmenopausal patients: assessment by PET/CT. J Nucl Med 2004;45:266–71.
[10] Habiba MA, Bell SC, Al-Azzawi F. The effect of hormone replacement therapy on the immunoreactive concentrations in the endometrium of oestrogen and progesterone receptor, heat shock protein 27, and human beta-lactoglobulin. Hum Reprod 2000;15:36–42.

資料 12

資料(13)

Ann Nucl Med (2008) 22:73–77
DOI 10.1007/s12149-007-0075-2

CASE REPORT

Distinctive FDG and FES accumulation pattern of two tamoxifen-treated patients with endometrial hyperplasia

Tetsuya Tsujikawa · Hidehiko Okazawa
Yoshio Yoshida · Tetsuya Mori · Masato Kobayashi
Tatsuro Tsuchida · Yasuhisa Fujibayashi

Received: 2 March 2007 / Accepted: 13 August 2007

Abstract 16α-[^{18}F]Fluoro-17β-estradiol (FES) is an estrogen receptor (ER) ligand used for the detection of ER-positive malignant tumors such as breast cancer. We recently reported the feasibility of combined FES- and 2-[^{18}F]fluoro-2-deoxy-D-glucose (FDG)-positron emission tomography (PET) scans for the differential diagnosis of endometrial tumors. ER expression measured by FES-PET was preserved in endometrial hyperplasia, whereas ERs were assumed to be reduced in endometrial carcinoma with accelerated glucose metabolism measured by FDG-PET. We report two postmenopausal patients under suspicion of endometrial carcinoma on the basis of cytology and/or magnetic resonance imaging (MRI), who were on tamoxifen treatment since undergoing surgery for breast cancer. Pelvic MRI suggested endometrial carcinomas, whereas FDG- and FES-PET showed no abnormal tracer accumulation. A postoperative histopathologic examination revealed that the lesions were endometrial hyperplasias with no malignant findings. FES-PET enables us to evaluate the ERα expression of endometrium noninvasively, whereas the evaluation of ER expression using FES-PET requires careful attention regarding the influence of hormonal therapy because tamoxifen greatly affects FES accumulation of even endometrial hyperplasia, which should be an FES-avid lesion.

Keywords Endometrial hyperplasia · Estrogen receptor · FES-PET · FDG-PET · Tamoxifen

T. Tsujikawa (✉) · H. Okazawa · T. Mori · M. Kobayashi · Y. Fujibayashi
Biomedical Imaging Research Center, University of Fukui, 23-3 Matsuoka-Shimoaizuki, Eiheiji-cho, Fukui 910-1193, Japan
e-mail: awaji@u-fukui.ac.jp

Y. Yoshida
Department of Gynecology, University of Fukui, Fukui, Japan

T. Tsuchida
Department of Radiology, University of Fukui, Fukui, Japan

Introduction

Endometrial hyperplasia is generally considered to represent the incipient stage of endometrial carcinoma [1]. It has been reported that the presence of continuous and excessive estrogen exposure associated with factors such as exogenous estrogen therapy, anovulatory cycles, polycystic ovary syndrome, and obesity would increase the incidence rate of endometrial hyperplasia and carcinoma. Positron emission tomography (PET) is a biologic imaging modality which can present an image of physiologic function. PET with 2-[^{18}F]fluoro-2-deoxy-D-glucose (FDG) can reflect glucose metabolism and activity of lesions including malignant tumors. FDG-PET is used for the evaluation of gynecologic malignancies in preoperative staging, postsurgical monitoring, and surveillance for recurrence [2]. On the other hand, 16α-[^{18}F]fluoro-17β-estradiol (FES) is an ^{18}F-labeled compound of estradiol (E2) which is the most bioactive type of estrogens. FES-PET enables us to evaluate the estrogen receptor (ER) density of a lesion and is usually used for the detection and management of ER-positive malignant tumors such as breast cancer [3–8]. We recently reported the feasibility of combined FES- and FDG-PET scans for the differential diagnosis of endometrial tumors [9]. The ER expression measured by FES-PET was pre-